Species Sensitivity to Hydrologic Whiplash in The Tree-Ring Record of the High Sierra Nevada

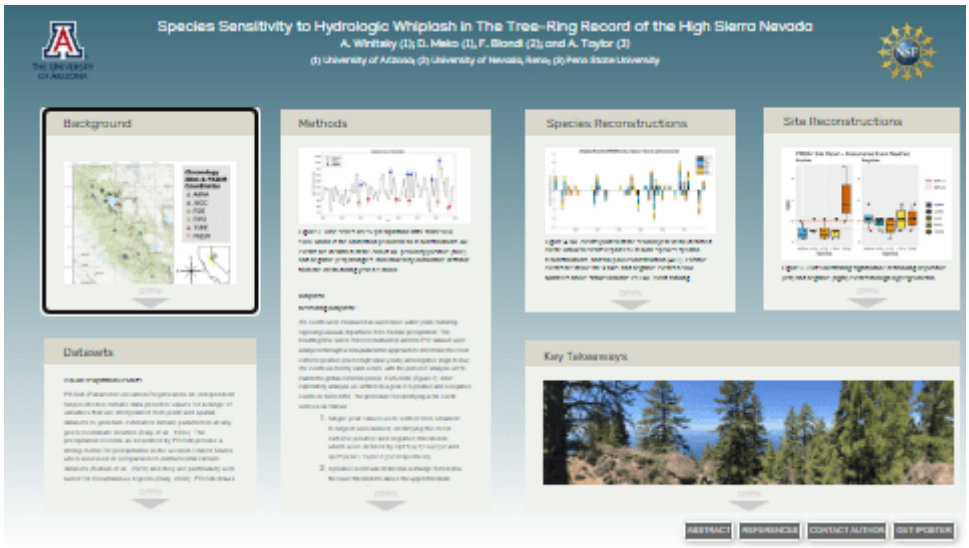

A. Winitsky (1); D. Meko (1), F. Biondi (2); and A. Taylor (3)

(1) University of Arizona; (2) University of Nevada, Reno; (3) Penn State University

PRESENTED AT:

Frontiers in Hydrology

BACKGROUND

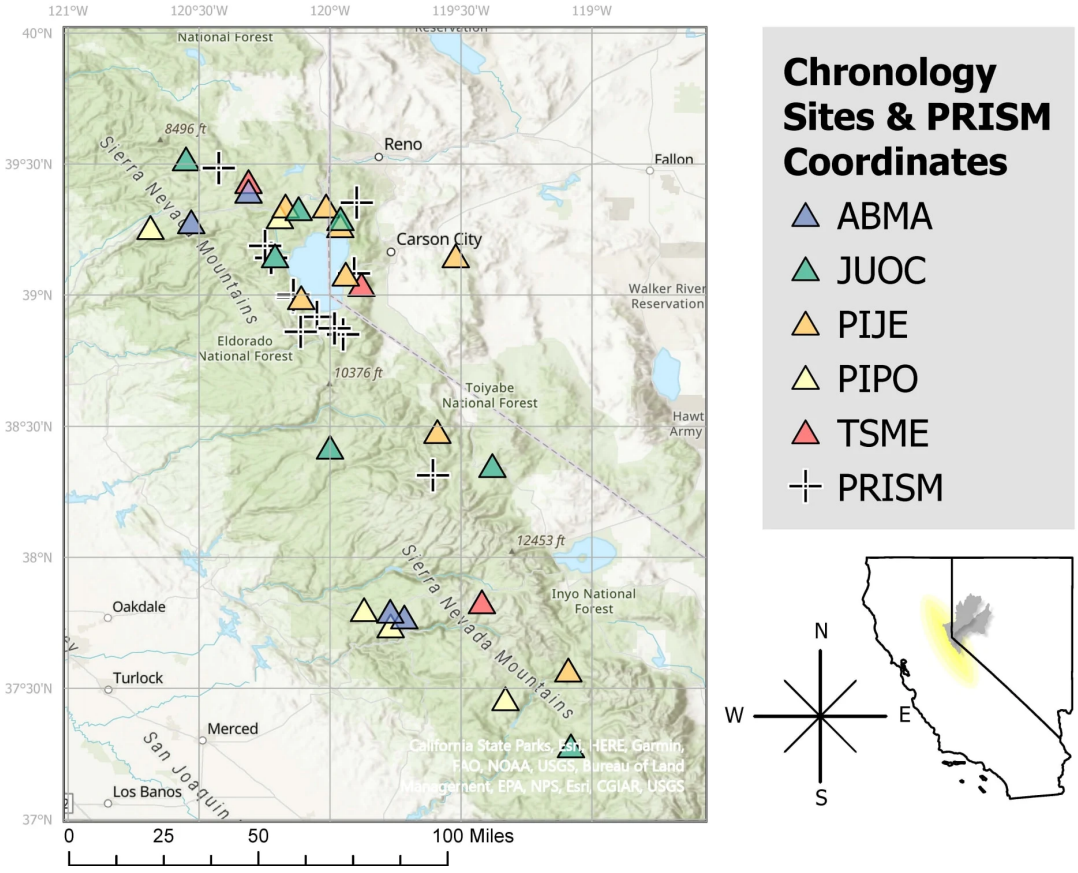

Figure 1. Regional map showing chronology sites color coded by species and coordinate locations used for PRISM water-year precipitation interpolation.

Introduction

Year-to-year variability of precipitation and temperature has significant consequences for water management decision making. “Whiplash” (WL) is a term which describes this variability at its most severe, referring to consecutive events in which the hydroclimate switches between extremes. Tree-rings in semi-arid environments like the Truckee-Carson River Basin (California/ Nevada watersheds with headwaters in the central Sierra Nevada) provide proxy records of hydroclimate as their annual growth is tied directly to climate limitations such as water availability (e.g., Biondi and Meko 2019), and therefore the practice of dendrochronology is useful for contextualizing long-term annualized climate variability (Meko et al. 2011). However, persistence in the total-ring width as a result of biological carryover processes can obscure records of WL events by supporting or suppressing growth in subsequent years (Fritts 1976).

In this analysis, we seek to determine:

1. **Do tree-ring reconstructions of annual precipitation in the TCRB identify whiplash in the observed precipitation record?**
2. **Are there differences in the tracking and recognition of whiplash events among species?**

Study Area/Climate

Watershed characteristics of the TCRW have led the Bureau of Reclamation (2015) to describe the management of the Truckee River as a “zero-sum game for water.” Climate variability is an integral characteristic of the TCRW, where seasonal climate fluctuates widely annually driven by large-scale oceanic and atmospheric patterns which result in hot dry summers and cold wet winters (Pandey, 1999; Mason and Goddard, 2001; Biondi and Meko 2019). However, recent studies have found that the interannual precipitation regime has become increasingly volatile since the mid-20th century, characterized by high intensity events and dry periods (Dettinger, 2011; Berg and Hall, 2015; Swain et al., 2018; Zamora Reyes et al. 2021). The increasing complexity of interannual precipitation in the region coupled with the annual fluctuations typical of the climate system make water management an increasingly challenging task. It is in this context that understanding the baseline frequency of annual WL events through dendrochronology can support water management efforts.

DATASETS

PRISM Precipitation Records

PRISM (Parameter-elevation Regressions on Independent Slopes Model) climate data provides values for a range of variables that are interpolated from point and spatial datasets to generate estimated climate parameters at any given coordinate location (Daly et al., 1994). The precipitation records as described by PRISM provide a strong metric for precipitation in the western United States when assessed in comparison to instrumental climate datasets (Buban et al., 2020) and they are particularly well suited for mountainous regions (Daly, 2006). PRISM draws from a wide network of climate stations and provides records back to 1895; however, due to the sporadic nature of data availability in the instrumental record during the early part of the 19th century, for this analysis we chose to limit precipitation records to a start year of 1920.

The particular PRISM time series selected as the primary variable for reconstruction is water-year (Oct-Sep) total precipitation averaged over coordinate points corresponding to 12 snow-monitoring locations throughout the TCRB (Figure 1). From this point forward this precipitation series will be referred to as P12.

Tree-Ring Chronologies

Five snow-adapted conifer species *(Abies magnifica* (ABMA), *Juniperus occidentalis* (JUOC), *Pinus ponderosa* (PIPO), *Pinus jeffreyi* (PIJE), and *Tsuga mertensiana* (TSME)) were selected for this analysis (Figure 1). Species were required to meet specific requirements for spatial representation and time coverage. Data files of measured total ring width were initially sourced from the public-domain data set available through the International Tree-Ring Data Bank (Contributors of the ITRDB, accessed 2021), and further supplemented by contribution of the authors (Table 1). Highly diverse chronology lengths were trimmed to a start date of 1800; some site records began later. Individual cores that did not have RWI values in 1950 were removed from the model to ensure a minimum of overlap with the calibration period by 30 or more years.

Reconstruction

Chronologies were transformed into estimates of precipitation by distributed-lag stepwise regression models (e.g., Meko and Graybill 1995). Single-site models (29 models) were developed by individually regressing P12 on each chronology and its lags t-2 to t+2 years from the year of P12. Species-specific models (5 models) were developed by including all chronologies, with lags, of each species in the pool of potential predictors. An additional full-pool model (ALL) was developed that included all 29 chronologies and their lags in the pool. Before stepwise regression, the pool of potential predictors was reduced, if needed, by correlation screening against P12 to ensure that the number of potential predictors was no more than 1/5 the sample size (number of years) in the calibration period of the regression model. The stepwise regression was guided by a cross-validation stopping rule (Wilks 2019).

Table 1. Complete pool of predictor chronologies used in various tree-ring reconstructions of P12.

site code	species code	lat	lon	elev (m)	source	start year	end year
CA574	ABMA	37.77	-119.77	2180	ITRDB	1880	1991
CA589	ABMA	37.78	-119.73	2075	ITRDB	1880	1991
CA691	ABMA	39.42	-120.31	2478	ITRDB	1540	2015
CA696	ABMA	39.28	-120.53	2008	ITRDB	1799	2014
CA630	JUOC	38.42	-120	2591	ITRDB	-420	1999
CA631	JUOC	39.52	-120.55	1921	ITRDB	930	1999
CA632	JUOC	39.33	-120.12	2268	ITRDB	1010	1999
CA698	JUOC	39.15	-120.21	1809	ITRDB	1600	2014
DGS	JUOC	38.35	-119.38	2370	Biondi	-300	2000
IVJ	JUOC	39.28	-119.96	2563	Taylor	1142	2000
KAIM	JUOC	37.28	-119.08	2730	Meko	1140	2011
CA677	PIJE	39.34	-120.17	1688	ITRDB	1415	2010
CA678	PIJE	37.57	-119.09	2499	ITRDB	1304	2010
DLB	PIJE	38.99	-120.11	2004	Taylor	1306	2000
IVP	PIJE	39.27	-119.96	2332	Taylor	1305	2000
LEM	PIJE	39.34	-120.015	2008	Biondi	1542	2020
LSF	PIJE	38.48	-119.59	2416	Biondi	1474	2020
LTV	PIJE	39.15	-119.52	2006	Biondi	1418	2020
SSP	PIJE	39.08	-119.94	2132	Taylor	1190	1999
CA578	PIPO	37.8	-119.87	1722	ITRDB	1880	1990
CA583	PIPO	37.75	-119.77	1803	ITRDB	1880	1990
CA694	PIPO	39.2988	-120.1915	1975	ITRDB	1829	2014
CA695	PIPO	39.258	-120.6857	1537	ITRDB	1838	2014
CPRMTR	PIPO	39.27	-119.57	2507	Biondi	1474	2020
NOD	PIPO	37.46	-119.33	1539	Biondi	1539	2002
CA567	TSME	37.83	-119.42	2960	ITRDB	1880	1990
CA692	TSME	39.42	-120.31	2478	ITRDB	1615	2015
GPH	TSME	39.04	-119.88	2728	Taylor	1349	2000

METHODS

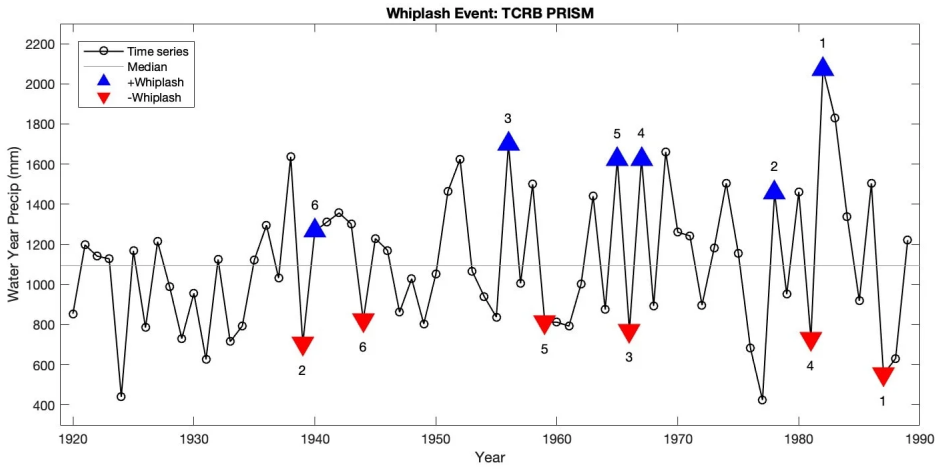

Figure 2. Time series of P12 precipitation data, from 1920 - 1989, which is the calibration period for all reconstructions. WL events are identified at the end of WL period by positive (blue) and negative (red) triangles, and ranked by cumulative distance from the mean during year n-1 and n.

Whiplash

Measuring Whiplash:

WL events were measured as successive water years featuring opposing unusual departures from median precipitation. The resulting time series from reconstruction and the P12 dataset were analyzed through a non-parametric approach to determine the most extreme positive (low to high value years) and negative (high to low) WL events as told by each series, with the period of analysis set to match the global common period; 1920-1989 (Figure 2). After exploratory analysis we settled on a goal of 6 positive and 6 negative events in 1920-1989. The procedure for identifying a WL event series is as follows:

1. Single year values were sorted from smallest to largest and ranked, identifying the most extreme positive and negative thresholds, which were defined by cp1=(s(1)+s(2))/2 and cp2=(s(n2) +s(n2-1))/2 respectively.

2. A positive event was defined as a change from below the lower threshold to above the upper threshold, and vice-versa for a negative event .

3. The thresholds were relaxed by collapsing them toward the median by 1 ranked value.

4. Steps 1-3 were repeated until some specified number of events were represented in the analysis period.

5. The process was repeated independently for each time series. Because events were identified separately for each series, the thresholds for inclusion to reach the desired event tally varied among series.

Hypergeometric Distribution

Determining the significance events through hypergeometric distribution:

Statistical significance of the match of WL events in each reconstructed series and the P12 was assessed through hypergeometric distribution, which has been applied in past studies to examine relationships in climate and hydrologic variables (e.g., Dracup and Kahya, 1994; Meko and Graybill, 1995). If there are m=6 events in the precipitation series for the N=70 year analysis period, the hypergeometric distribution gives the probability of drawing x of those events in k attempts by chance alone. In our application, we treat the events in the reconstructed series as the k "attempts." For the reconstructions, k=6 or k=7, because the collapsing-quantile procedure outlined earlier cannot guarantee exactly 6 events.

SPECIES RECONSTRUCTIONS

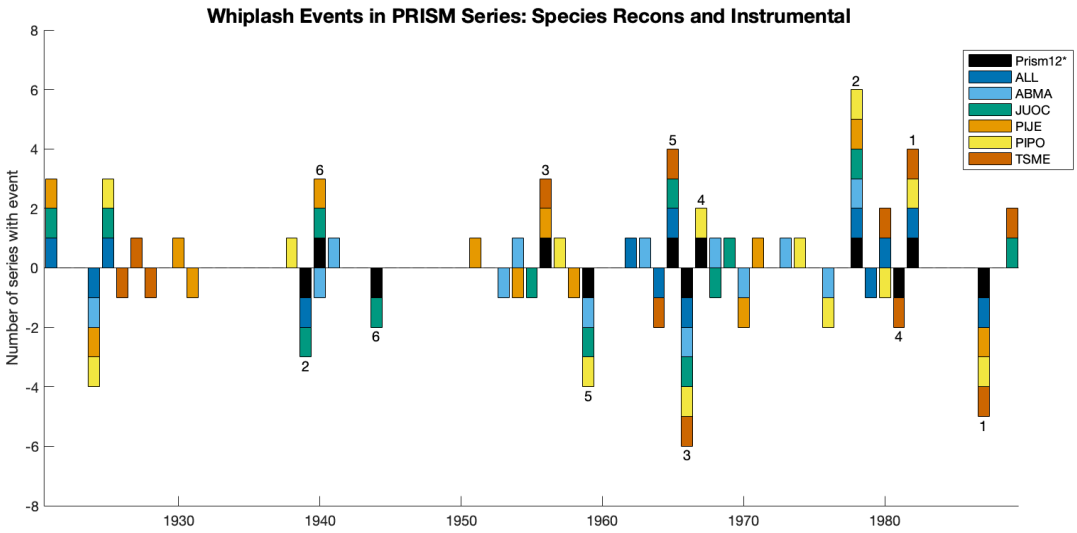

Figure 4. WL events plotted at the second year of an identified event. Stacked events report P12 record, species-specific reconstructions, and full-pool reconstruction (ALL). Positive events are above the x axis, and negative events below. Numbers above stacks indicate P12 WL event ranking.

Events:

Figure 4 illustrates the WL events identified by P12 and reconstructed series. Tracking of P12 WL events varied over the species-specific and full-pool reconstructions.

- Some events were more consistently tracked by numerous reconstructions including a positive WL event in 1977-1978 and a negative WL event in 1965-1966 which were tracked by all but one model.
- Some WL events were missed by most reconstructions, though no P12 WL event was missed by all models.
- Tracking ability has no clear association with severity of WL event. The highest ranked P12 WL events were not tracked at the highest rates. The second and third ranking WL events had the highest tracking in positive and negative P12 WL events respectively.

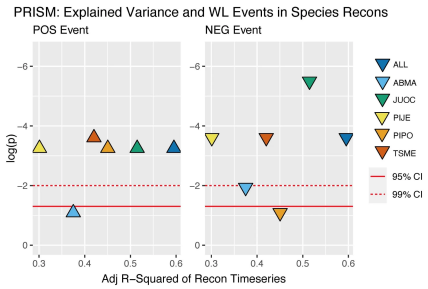

Figure 3. Plots illustrating positive (left) and negative (right) WL event significance as described through hypergeometric analysis and total explained variance (r2) for time series models of P12.

Hypergeometric Distribution:

A positively trending relationship between R^2 and log(p) would indicate that the WL events captured are directly related to overall explained variance. However, in a simple linear regression model of R^2 against log(p), the slope was not significant at 95% CI for either positive or negative WL events (Pr(>|t|) = 0.578 and 0.579 respectively), and there is no obvious pattern in the scatterplots. (Figure 3).

- ABMA and PIPO models correlate least with P12. However, while ABMA failed to track either positive or negative P12 WL with 99% significance, PIPO's tracking of events was on par with the success of other models including those with highest overall explained variance.
- JUOC, TSME, PIPO and ALL tracked both positive and negative P12 WL events at 99% significance.
- PIJE tracked positive WL events better (>99%CI) than negative events (<95%CI).

Table 2. Summary statistics of reconstructions of P12 from species-specific reconstructions and from full-pool reconstruction (ALL).

Recon	Chrons	Start Year	End Year	R2	R2adj	F	pF	REcv	RSME
ABMA	CA696P1 CA691P1 CA574P1 CA574 CA589P1 CA696	1880	1989	0.430	0.375	7.800	2.85E-06	0.384	276.220
ALL	DGS (JUOC) CA574 (PIJE) CA567P1 (TSME)	1879	1989	0.613	0.595	34.327	2.04E-13	0.583	227.276
JUOC	DGS KAIM IVJN2 CA630	1802	1997	0.540	0.515	21.421	1.02E-11	0.498	253.836
PIJE	CA677 CA678 LSFP1 LEM LSF	1802	1997	0.486	0.450	13.622	2.36E-09	0.426	271.409
PIPO	CA578 CA694P1	1880	1989	0.321	0.301	15.634	2.77E-06	0.247	305.411
TSME	CA692P1 CA567P1 GPH GPHP2 CA692N2	1879	1989	0.463	0.420	10.855	1.48E-07	0.409	270.588

SITE RECONSTRUCTIONS

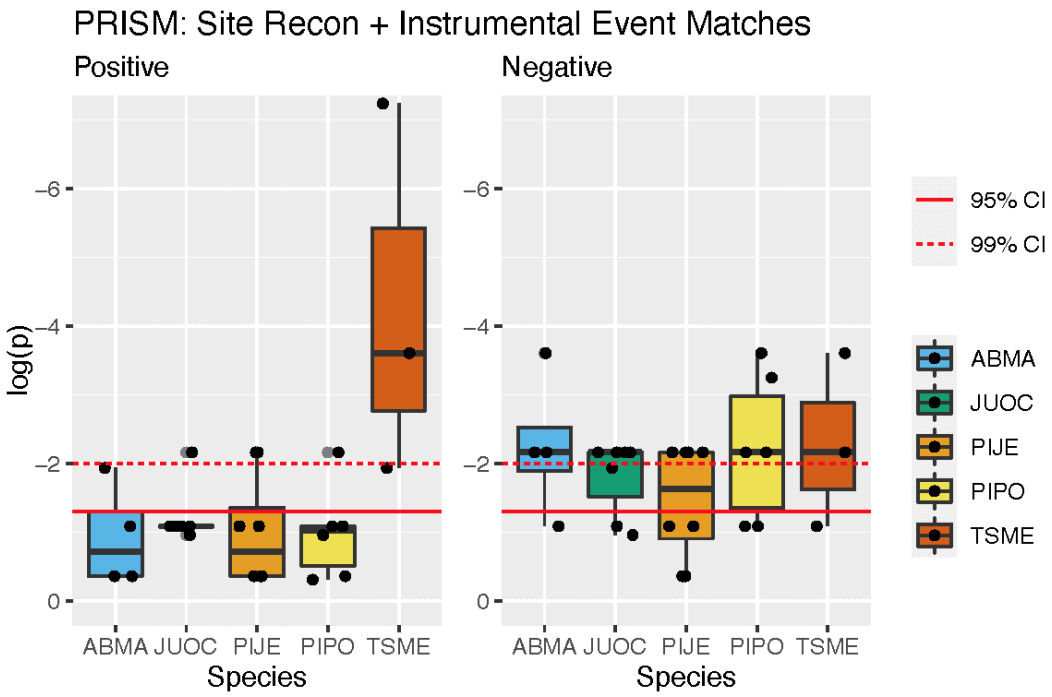

Figure 5. Plots illustrating significance of tracking of positive (left) and negative (right) events through hypergeometric analysis for single-site models. Species color coded. Each box plot summarizes distribution of p-values for tracking for chronologies of that species.

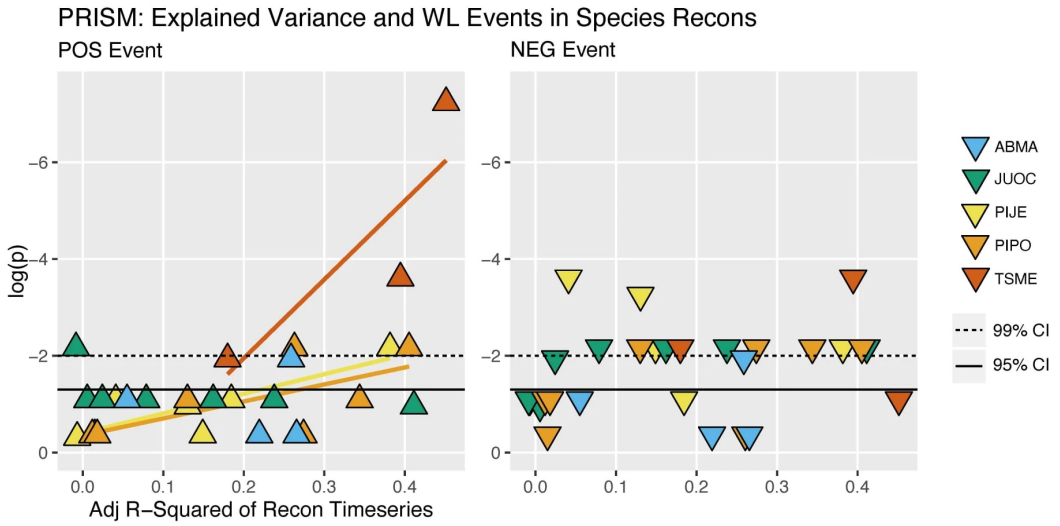

Figure 6. WL event significance and explained variance for site-specific reconstructed series. Plotting convention as in Figure 3. Trendlines are shown where sites grouped by species have a significant linear trend, and are colored to match corresponding species.

Hypergeometric Distribution:

Box-plots in Figure 5 showcase the distribution of P12 WL event significance for single-site reconstructions. Overall, negative events were tracked more often than positive events.

- All species showed some variation among sites in their tracking of P12 WL events.
- Positive P12 WL events were tracked poorly (<50% sites at 95% CI) by all species except TSME, which tracked them well (all sites at >95% CI).
- Negative P12 WL events were tracked well (PIJE >50% sites at 95% CI, all other species >50% sites at a 99% CI).

In Figure 6 single-site reconstructions of three species (TSME, PIPO, and PIJE) show a positive linear trend between R^2 and log(p) in positive WL event series, while the remaining two positive and all negative series do not.

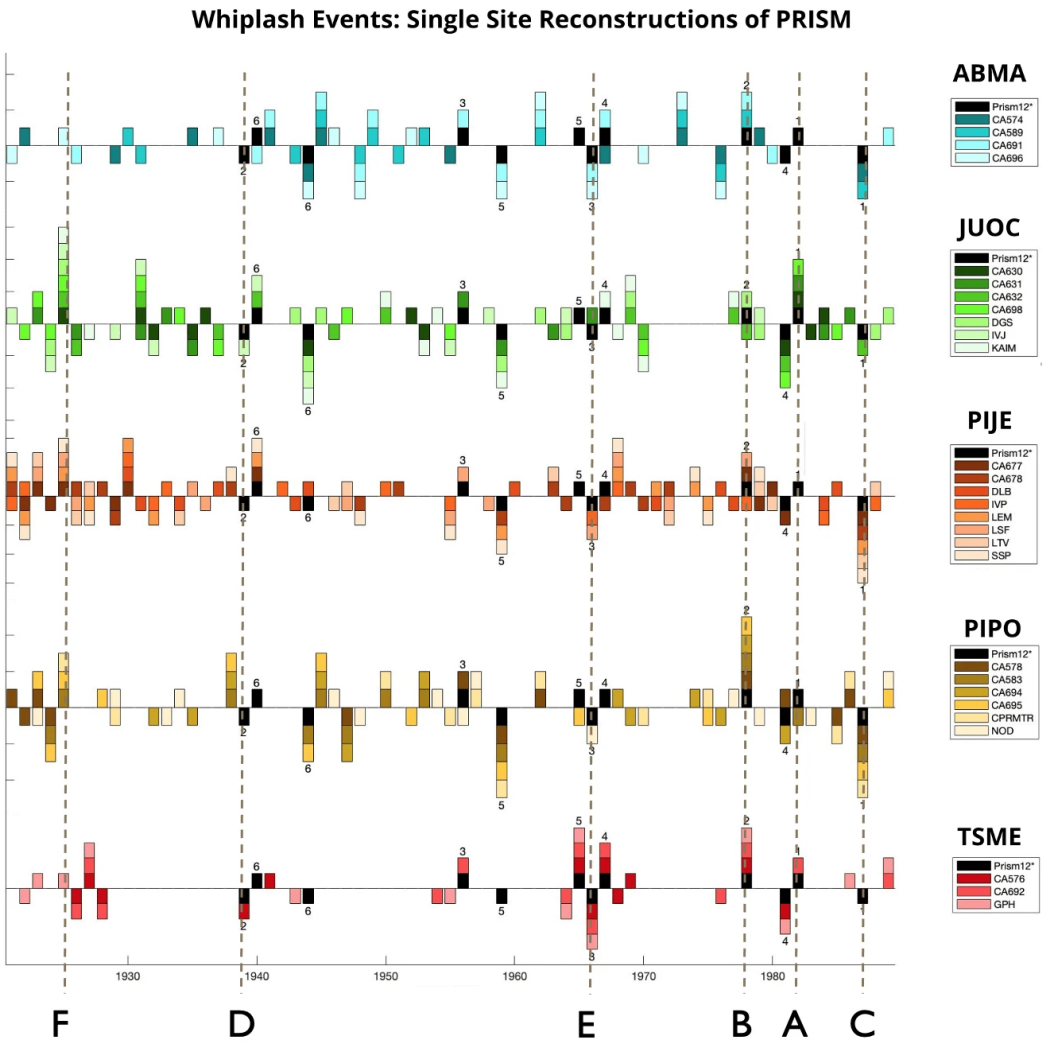

Figure 7. WL events for single-site reconstructions grouped by tree species. Plotting convention as in Figure 4. Stacked events are color-coded by chronology site code (see Table 1).

Events:

Patterns in event tracking described below relate to particular WL events identified in Figure 7.

- **A**) The most severe Positive P12 WL event was tracked by less than <50% of sites across all species.
- **B**) The second most severe Positive P12 WL event was tracked by >=50% of sites by all species except JUOC and PIJE
- **C**) The most severe Negative P12 WL event was tracked by >50% of PIJE and PIPO and <50% by other species.
- **D**) The second most severe Positive P12 WL event was tracked by <50% of sites by all species.
- **E**) Three concurrent WL years were tracked >50% by TSME and <50% by all other species.
- **F**) Post-drought recovery in 1925, which did not qualify as P12 WL due to near-median precipitation in 1924, was reported as as WL by >=50% of JUOC, PIJE, and PIPO sites. Some other hydrologic time series we investigated (e.g., Northern Sierra 8 Station Precipitation (CDEC, 2021)) do record this two-year period as a WL event.

KEY TAKEAWAYS

Figure 8. PIJE collection site Shakespeare Point (code SSP), above east shore of Lake Tahoe.

Outcomes

Tree-ring reconstructions of P12 by five conifer series track a significant number of WL events, and tracking varies among species.

- Single-site reconstructions track negative P12 WL events well, while only TSME tracks positive events well.
- Species-specific reconstructions of P12 often display non-random tracking of positive and negative WL events (4/5 species in each), where some events had more matches by reconstructions than others, with no event tracked by all series. A higher event ranking did not always correspond to better tracking.
- The full-pool reconstruction tracks positive and negative WL significantly at a 99% CI.
- Traditional metrics of skill (e.g., R^2) are not directly related to WL tracking outcomes.

Future Directions

Sensitivity Analysis:

- Factors in reconstruction procedures such as inclusion or exclusion of lagged years in the predictor pool, choice of analysis period, choice of hydrologic variable, standardization method and use of standardized vs residual chronologies could affect WL outcomes in reconstructed series.
- Alternatives to the nonparametric approach to determining WL events in favor of other mathematical evaluations could be considered.
- Thresholds were set with a goal of the same number of WL events in each series for the analysis period; this is only one of many possible approaches to WL classification.

Opportunities for further analysis:

- Trends in thresholds regarding positive vs negative events, event severity, etc.
- Climate in years defined as WL by reconstructions or chronologies.

- Climate impacts on WL tracking including effects of multi-year drought or pluvial periods preceding P12 WL event years or interannual or seasonal variability.

Concluding thoughts

The results of this study suggest that ring-width indices from the assessed conifer species in the snow-belt of the Sierra Nevada are often able to record consecutive years of opposing extreme precipitation and report such events through derived models. Residual effects of a preceding year's drought or pluvial do not necessarily suppress records of WL, though sensitivity to precursor conditions in tracking of WL events may differ across species.

In some cases, tree ring reconstructions track known WL events at a significant rate even with relatively low explained variance by the model overall. The findings suggest that it may be unwise to assume that WL events will be well-tracked just because a reconstruction model has a high explained variance. The methodologies developed for this study could assist in testing models for their sensitivity to WL events.

Acknowledgements

This work was supported by National Science Foundation Awards #1903535 (Meko) and #1903561 (Biondi).

ABSTRACT

Year-to-year variability of precipitation and temperature has significant consequences for water management decision making. “Whiplash” is a term which describes this variability at its most severe, referring to events at various timescales in which the hydroclimate switches between extremes. Tree-rings in semi-arid environments like the Truckee-Carson River Basin (California/Nevada watersheds with headwaters in the Sierra Nevada) can provide proxy records of hydroclimate as their annual growth is tied directly to limitations in water-year rainfall and temperature. In this study, a pool of total ring width indices from five snow-adapted conifer species (*Abies magnifica*, *Pinus jeffreyi*, *Juniperus occidentalis*, *Tsuga mertensiana*) were used to develop single-species standardized reconstructions of annualized hydroclimate phenomena using stepwise forward linear regression. A nonparametric analysis approach was then used to determine positive and negative whiplash events in reconstructed and instrumental hydroclimate variables. Multivariate analysis of the resulting timeseries datasets illustrates relationships between reconstructions and recorded whiplash events and allows for determination of patterns in tree-ring growth response. Individualized species response provides analytical and methodological insight for past and potential climate reconstruction using similar approaches, as well as possible species growth response to future increases in hydroclimate variability brought on by climate change.

REFERENCES

1. Berg, N., & Hall, A. (2015). Increased Interannual Precipitation Extremes over California under Climate Change. Journal of Climate, 28(16), 6324–6334. https://doi.org/10.1175/JCLI-D-14-00624.1
2. Biondi, F., & Meko, D. M. (2019). Long−Term Hydroclimatic Patterns in the Truckee−Carson Basin of the Eastern Sierra Nevada, USA. 55. https://doi.org/10.1029/2019wr024735
3. Buban, M. S., Lee, T. R., & Baker, C. B. (2020). A Comparison of the U.S. Climate Reference Network Precipitation Data to the Parameter-Elevation Regressions on Independent Slopes Model (PRISM). Journal of Hydrometeorology, 21(10), 2391–2400. https://doi.org/10.1175/JHM-D-19-0232.1
4. California Data Exchange Center (CDEC). (2021) Northern Sierra 8 Station Chronological Monthly Precipitation. Retrieved January 2022, from https://cdec.water.ca.gov/cgi-progs/precip1/8STATIONHIST
5. Daly, C., Neilson, R. P., & Phillips, D. L. (1994). A Statistical-Topographic Model for Mapping Climatological Precipitation over Mountainous Terrain. Journal of Applied Meteorology and Climatology, 33(2), 140–158. https://doi.org/10.1175/1520-0450(1994)033<0140:ASTMFM>2.0.CO;2
6. Daly, C. (2006). Guidelines for assessing the suitability of spatial climate data sets. International Journal of Climatology, 26(6), 707–721. https://doi.org/10.1002/joc.1322
7. Dettinger, M. (2011). Climate Change, Atmospheric Rivers, and Floods in California – A Multimodel Analysis of Storm Frequency and Magnitude Changes1. JAWRA Journal of the American Water Resources Association, 47(3), 514–523. https://doi.org/10.1111/j.1752-1688.2011.00546.x
8. Dracup, J. A., & Kahya, E. (1994). The relationships between U.S. streamflow and La Niña Events. Water Resources Research, 30(7), 2133–2141. https://doi.org/10.1029/94WR00751
9. Fritts, H. C. (1976). Tree Rings and Climate (567 pp.). Academic Press. https://doi.org/10.1016/B978-0-12-268450-0.50006-9
10. Mason, S. J., & Goddard, L. (2001). Probabilistic Precipitation Anomalies Associated with ENSO. Bulletin of the American Meteorological Society, 82(4), 619–638. https://www.jstor.org/stable/10.2307/26215541
11. Meko, D., & Graybill, D. A. (1995). Tree-Ring Reconstruction of Upper Gila Rwer Discharge1. JAWRA Journal of the American Water Resources Association, 31(4), 605–616. https://doi.org/10.1111/j.1752-1688.1995.tb03388.x
12. Meko, D. M., & Woodhouse, C. A. (2011). Application of Streamflow Reconstruction to Water Resources Management. In M. K. Hughes, T. W. Swetnam, & H. F. Diaz (Eds.), Dendroclimatology: Progress and Prospects (pp. 231–261). Springer Netherlands. https://doi.org/10.1007/978-1-4020-5725-0_8
13. Pandey, G. R., Cayan, D. R., & Georgakakos, K. P. (1999). Precipitation structure in the Sierra Nevada of California during winter. Journal of Geophysical Research: Atmospheres, 104(D10), 12019–12030. https://doi.org/10.1029/1999JD900103
14. Reclamation. (2016). Chapter 9: Truckee River Basin. Report to United States Congress, US Department of the Interior and Bureau of Reclamation. (27 pp.) https://www.usbr.gov/climate/secure/docs/2016secure/2016SECUREReport-chapter9.pdf
15. Swain, D. L., Langenbrunner, B., Neelin, J. D., & Hall, A. (2018). Increasing precipitation volatility in twenty-first-century California. Nature Climate Change, 8(5), 427–433. https://doi.org/10.1038/s41558-018-0140-y
16. Wilks, D. S. (2019). Statistical Methods in the Atmospheric Sciences (Fourth ed.). Cambridge, MA: Slsevier. (818pp.).
17. Zamora-Reyes, D., Black, B., & Trouet, V. (n.d.). Enhanced winter, spring, and summer hydroclimate variability across California from 1940 to 2019. International Journal of Climatology. https://doi.org/10.1002/joc.7513